IEEE Access
Multidisciplinary | Rapid Review | Open Access Journal

Received August 3, 2020, accepted August 8, 2020, date of publication August 13, 2020, date of current version August 25, 2020.

Digital Object Identifier 10.1109/ACCESS.2020.3016377

Outage Probability and Throughput Analyses in Full-Duplex Relaying Systems With Energy Transfer

JIAMAN LI, LE CHUNG TRAN, (Senior Member, IEEE), AND FARZAD SAFAEI, (Senior Member, IEEE)
School of Electrical, Computer, and Telecommunications Engineering, University of Wollongong, Wollongong, NSW 2522, Australia
Corresponding author: Jiaman Li (jl797@uowmail.edu.au)

ABSTRACT In this article, we consider a dual-hop full-duplex (FD), amplify-and-forward, orthogonal frequency division multiplexing (OFDM) relaying network, where the relay operates based on a time-switching architecture to harvest energy from radio frequency signals. We use a polarization-enabled digital self-interference cancellation (PDC) scheme to cancel the self-interference signal at the relay in order to achieve FD communications. The paper provides a comprehensive analysis of the system performances in terms of outage probability and throughput over multipath Rayleigh fading channels. Furthermore, the optimal time split between the duration of energy harvesting and signal transmission to maximize the system throughput is numerically calculated. We also derive the asymptotic lines to simplify the expressions of outage probability and throughput at high transmit signal-to-noise ratios (SNR). Our analysis and simulation results show that the proposed FD relaying system by utilizing a proper time split fraction can boost the system throughput significantly over an appreciable range of transmitting SNR values, compared to half-duplex (HD) relaying systems.

INDEX TERMS Dual-hop systems, full-duplex relaying, energy harvesting, throughput, outage probability, OFDM.

I. INTRODUCTION

The conventional energy-constrained wireless networks, such as wireless sensor networks, have a limited lifetime. For the energy-limited sensors, recharging or replacing batteries is periodically performed to sustain network operations, which is costly, time-consuming, and sometimes infeasible due to some physical limitations, such as hazardous environments. Wireless energy harvesting (EH) techniques provide a solution to realize the long-term operation of the sensors in this kind of scenario. Some preliminary works [1]–[3] rely on natural energy sources, such as solar, wind, and thermoelectric effects to provide EH. However, these sources cannot be controlled and the harvesting requires peripheral EH equipment. Recently, EH techniques using radio frequency (RF) signals and electromagnetic (EM) induction to achieve energy transfer have attracted significant interest because the man-made RF signal and EM induction can steadily deliver energy to the destination to provide a reliable energy supply. In [4], the authors consider a system with a single transmit antenna and multiple receive antennas, where the energy is transferred to the destination through RF signals. The diversity combining technique is used to improve the EH performance. The works in [5]–[7] propose methods that use the EM induction mechanism to achieve EH, where the EM energy conversion is based on Faraday's law. Wireless EH from an EM induction requires the designing of EM power-generators and usually works in a short distance while RF signals can readily carry both energy and information at the same time to the receiver at distance. Thus, the EH from RF signals can cost-effectively prolong the lifetime of wireless communications systems.

The cooperative communication is widely adopted to improve the system performances and extend the coverage of wireless networks. In [8], a source transmitting information to destination through either the direct source-to-destination link or the assistance of K relays is researched. The use of the direct link can provide spatial diversity and increase the spectral efficiency of the relaying system. However, the direct link is not always available in practice. Therefore, numerous works, such as [9]–[11], have researched relaying systems without a direct link between the source and the destination, which is applicable to the situation when the

The associate editor coordinating the review of this manuscript and approving it for publication was Theofanis P. Raptis.

distance between the source and the destination is large so that the destination is not within the coverage area of the source and when the direct link is in heavy shadowing due to obstructions. In the cooperative communication, the two most commonly used relaying protocols include the amplify-and-forward (AF) protocol and the decode-and-forward (DF) protocol. In the AF protocol, the relay node amplifies the received signal from the source and then forwards to the destination [8], [10], [12]–[15] while the DF protocol decodes the received signal at the relay before forwarding [8], [9], [14], [16], [17]. Combining relaying systems with EH has also seen an upsurge of research interests recently. In [12], the authors consider a HD system in which the relay transmits and receives information in different time slots over Rayleigh flat-fading channels. They derive the analytical expression of the outage probability and the ergodic capacity to determine the throughput performance and investigate the effect of various system parameters on the performance of wireless EH relaying systems. In [9], a relay selection protocol for EH systems with no direct link between the source and destination is proposed, where the highest energy signal is chosen by the relay for harvesting energy. The system performance in terms of outage probability is researched over Rayleigh fading channels. Later in [13], the average throughput is analyzed for the EH cooperative system by considering both continuous-time and discrete-time EH protocols over Rician fading channels. In [15], the non-linear energy harvester at the relay is studied over Nakagami-m fading channels. The work in [16] considers the N^{th} best-relay selection scheme in EH systems, where the destination selects the relay based on the N^{th}-order channel gains. The authors evaluate the exact outage probabilities of time switching-based relaying (TSR) protocol and power splitting-based relaying (PSR) protocol. In [11], the authors investigate the achievable information rate in the MIMO-OFDM networks with a wireless power relay. However, it is worth pointing out that all these works are limited to the HD mechanism, i.e., the relay node cannot receive and transmit information simultaneously in the same frequency band.

The HD relaying architecture is widely used in conventional wireless networks due to its simpler system design. However, HD transmission leads to a loss of spectrum efficiency. To overcome this problem, the FD architecture is proposed to achieve concurrent transmission and reception in the same band. In [14], the throughput performance and the optimal time splitting in the FD relaying system with wireless power transfer for single-carrier communication are studied. In [8], a partial relay selection scheme is proposed to implement FD transmission, where the relay having the best-receiving information signal is selected. However, these works neither consider multipath frequency-selective fading channels nor any specific self-interference cancellation (SIC) method. The work in [18] simulates the throughput and BER performances of a FD EH relaying system in comparison with those of a HD EH relaying system. However, [18] does not derive the analytical expressions of outage probability and throughput and only considers flat-fading channels with a single carrier system.

To the best of the authors' knowledge, for the first time, the OFDM technique and the oblique projection method are adopted in this work to achieve a FD transmission in EH relaying systems. This work (i) provides a comprehensive analysis of the system performances in terms of outage probability and throughput; (ii) considers frequency-selective fading with the application of OFDM; and (iii) derives the optimal time splitting factor between the duration of energy harvesting and that of signal transmission to maximize the system throughput.

The main target of our research is to focus on a dual-hop scenario where the direct link from the source to destination is not available due to obstructions or a large distance. An intermediary relay is deployed, which is powered by the wireless RF signal in the first phase and implements simultaneous transmission and reception at the same frequency band in the second phase. This system model can be potentially applied in various energy-constrained scenarios. For example, in wireless sensor networks, a node with a fixed power supply wants to send information to a sensor. The direct link between them is interrupted by obstacles. So, the node needs an intermediary sensor to assist its information transmission. To prolong the lifetime of the intermediary sensor, the EH sensor is used instead of a battery-limited sensor. Another example is that, a source station wants to transmit data to a destination station which is far away from the source. A relay node with a fixed energy supply is unavailable due to the rugged environment. In this scenario, deploying an EH relay is a more convenient solution to help information transmission from the source to the destination. As for the SIC, we consider the combination of antenna polarization and oblique projection, i.e., the polarization-enabled digital self-interference cancellation scheme, to eliminate the self-interference (SI) at the relay. In order to demonstrate the outage probability and throughput of our proposed system, the performance of the HD EH relaying system in [12] is used as a benchmark.

The main contributions of the paper includes:

- We present analytical expressions for the outage probability and the system throughput. Specifically, the expressions of the outage probability are derived using two methods. Our findings show that, the method that considers the product distribution of the source-relay channel and relay-destination channel is more accurate at low SNRs, both methods are accurate at high SNRs.
- The optimal time split between the EH and information exchange phases is calculated numerically to maximize the system throughput. The outage probability decreases along with the increase of the EH duration.
- A PDC scheme is used at the relay to cancel the SI signal. The results show that, with this cancellation technique, the throughput of our FD relaying system can be nearly doubled, compared to that of the HD relaying system.

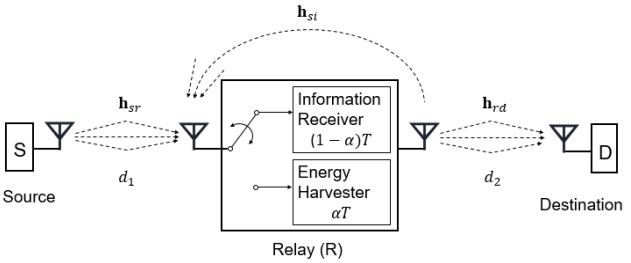

FIGURE 1. System model with multipath propagation.

- By comparing the FD and HD relaying architectures, the paper demonstrates that FD relaying can boost the system throughput with a proper time split and transmit SNR. Although HD relaying outperforms the FD relaying in terms of outage probability, the performance gap gradually diminishes when the time split factor is large.
- At a high transmit SNR, we simplify the expressions for the outage probability and the system throughput to obtain the corresponding asymptotic lines.

The rest of this article is organized as follows. Section II introduces the system model of our FD EH relaying system and the theory of using oblique projection to cancel the SI signals at the relay. Section III models EH and information transmission processes and illustrates the analytical expressions of the outage probability, throughput, and optimal time splitting. Section IV illustrates numerical results to validate the theoretical analyses and provides comparisons with a existing solution in the literature to demonstrate system performances.

II. FD RELAYING

A. SYSTEM DESCRIPTION

We consider a dual-hop AF relaying system with FD transmission and wireless power transfer, as shown in Fig. 1, in which the source (S) communicates with the destination (D) with the help of the relay (R) as the direct link does not exist. The source and destination are equipped with one orthogonal dual-polarized antenna while the relay is equipped with two orthogonal dual-polarized antennas [19], i.e., one for transmission and one for reception during the information transmission phase [20], [21]. The source node has a fixed energy supply while the relay only has a limited power supply and relies on EH from the source transmitting signals [12]. The EH model at the relay is assumed as a linear RF model [10], [12], which is applicable to the scenario when the input RF power is high [22], [23]. Besides, we adopt the OFDM technique that divides the total system bandwidth B into M sub-bands, which effectively produce M frequency-flat fading channels. At the relay, we adopt the PDC scheme to remove the SI signals in our FD system.

Let d_1 and d_2 be distance from S to R and from R to D. We use the model $\lambda_1 = d_1^{-\beta}$ and $\lambda_2 = d_2^{-\beta}$ to take into account path loss, where β denotes the path loss exponent. The channel coefficient vector of S−R is $\mathbf{h}_{sr} = [h_{sr,1}, \ldots, h_{sr,L}]$, R−D is $\mathbf{h}_{rd} = [h_{rd,1}, \ldots, h_{rd,L}]$, and the loop-back interference channel of the relay is $\mathbf{h}_{si} = [h_{si,1}, \ldots, h_{si,L}]$, where L is the number of multipath channels.

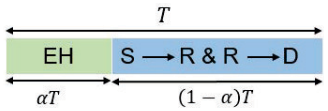

FIGURE 2. Time-switching EH architecture in a FD system.

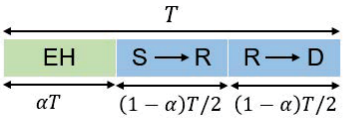

FIGURE 3. Time-switching EH architecture in a HD system.

TABLE 1. A summary of common notations.

Symbol	Description
$(.)^{\mathrm{T}}$	Transpose
$(.)^{\mathrm{H}}$	Hermitian transposition
$(.)^{-1}$	Inverse
.*	Element-wise multiplication
$\oplus$	Cyclic convolution
$\mathbb{E}.$	Expectation operator
$\lvert.\rvert$	Absolute value operator
fft	Fast Fourier transform
ifft	Inverse fast Fourier transform

To enable FD communication in our system, we adopt the FD time switching-based relaying (TSR) protocol in [14], [18], hence the whole communication process includes two phases as shown in Fig. 2. We define T (seconds) as the whole block time, and $0 < \alpha < 1$ as the time splitting factor, then the first duration αT is used for the relay to harvest energy. The remaining block time $(1-\alpha)T$ is used for information transmission. In particular, during this phase, the transmissions between the source and relay as well as the transmission between the relay and destination occur at the same time and in the same frequency band to increase spectral efficiency. For comparison, we also consider the HD EH relaying system with the TSR protocol as shown in Fig. 3, where the whole process is divided into three phases. The αT duration is used for EH, the first $(1-\alpha)T/2$ time is used for information transmission from the source to the relay, and the remaining $(1-\alpha)T/2$ time is used for information transmission from the relay to the destination.

B. PDC SCHEME

In this section, we introduce the theory of using the PDC scheme at the relay to eliminate the loop-back SI. The common notations are summarized in Table 1. The PDC scheme [19], [24] in our system requires the orthogonal dual-polarized antennas at the three nodes as well as the adoption of the oblique projection at the relay node.

We first introduce the Jones vector $\mathbf{J} = [\mathrm{J}_H \quad \mathrm{J}_V]^{\mathrm{T}} = [\cos(\varepsilon) \quad \sin(\varepsilon)\exp(j\delta)]^{\mathrm{T}}$ to express the signal polarization, where J_H represents the horizontal component, J_V represents the vertical component of the transmitted signal, $\varepsilon \in [0, \pi/2]$

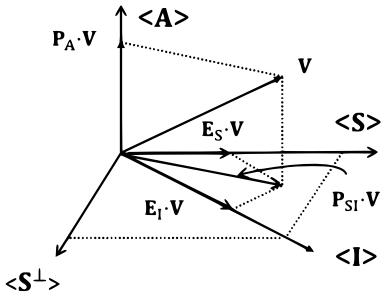

FIGURE 4. Three-way resolution of Euclidean space.

represents the polarization angle and $\delta \in [0, 2\pi]$ represents the phase difference between the vertical and horizontal components. The polarization states (PSs) of the desired information signal and the SI signal are denoted as $\mathbf{S}$ and $\mathbf{I}$ respectively.

$$\begin{aligned}\mathbf{S} &= \begin{bmatrix} S_1 & S_2 \end{bmatrix}^{\mathrm{T}} = \begin{bmatrix} \cos(\varepsilon_s) & \sin(\varepsilon_s)\exp(j\delta_s) \end{bmatrix}^{\mathrm{T}} \\ \mathbf{I} &= \begin{bmatrix} I_1 & I_2 \end{bmatrix}^{\mathrm{T}} = \begin{bmatrix} \cos(\varepsilon_i) & \sin(\varepsilon_i)\exp(j\delta_i) \end{bmatrix}^{\mathrm{T}}. \end{aligned} \quad (1)$$

where $\varepsilon_i, \varepsilon_s \in [0, \pi/2]$ and $\delta_i, \delta_s \in [0, 2\pi]$. In this article, we use dual-polarized antennas in communication. In the source-to-relay link, the PS $\mathbf{S}$ is used, while, in the relay-to-destination link, the PS $\mathbf{I}$ is used. It is worth noting that the re-transmitted signals from the relay to destination and the SI signal at the relay have the same PS $\mathbf{I}$.

Then, we introduce the vector $\mathbf{V}$ as the received signal at the relay, which includes both desired information signal received from the source node and its SI signal. In order to preserve the information signal and cancel the SI signal at the same time, the oblique projection is applied. As shown in Fig. 4, the orthogonal projection in the space $\langle \mathbf{A}, \mathbf{S}, \mathbf{S}^\perp \rangle$ is denoted as $\mathbf{P}$ with subscripts, which includes two components, $\mathbf{P}_{\mathrm{SI}}$ and $\mathbf{P}_{\mathrm{A}}$ projections. The oblique projection is denoted as $\mathbf{E}$ with the subscripts indicating the respective ranges. The well-known formula of an orthogonal projection with some range $\langle \mathbf{B} \rangle$ is $\mathbf{P}_{\mathrm{B}} = \mathbf{B}(\mathbf{B}^H\mathbf{B})^{-1}\mathbf{B}^H$, thus the signal $\mathbf{V}$ after the orthogonal projection onto the linear subspace $\langle \mathbf{S}\ \mathbf{I} \rangle$ is given by [24]

$$\mathbf{P}_{\mathrm{SI}} = \begin{bmatrix} \mathbf{S} & \mathbf{I} \end{bmatrix} \begin{bmatrix} \mathbf{S}^{\mathrm{H}}\mathbf{S} & \mathbf{S}^{\mathrm{H}}\mathbf{I} \\ \mathbf{I}^{\mathrm{H}}\mathbf{S} & \mathbf{I}^{\mathrm{H}}\mathbf{I} \end{bmatrix}^{-1} \begin{bmatrix} \mathbf{S}^{\mathrm{H}} \\ \mathbf{I}^{\mathrm{H}} \end{bmatrix}, \quad (2)$$

where the sub-spaces $\langle \mathbf{S} \rangle$ and $\langle \mathbf{I} \rangle$ are non-overlapping or disjoint. This orthogonal projection can be decomposed as

$$\mathbf{P}_{\mathrm{SI}} = \mathbf{E}_{\mathrm{S}} + \mathbf{E}_{\mathrm{I}}, \quad (3)$$

where $\mathbf{E}_{\mathrm{S}}$ and $\mathbf{E}_{\mathrm{I}}$ are two oblique projections with the respective ranges $\langle \mathbf{S} \rangle$ and $\langle \mathbf{I} \rangle$ and the respective null spaces $\langle \mathbf{I} \rangle$ and $\langle \mathbf{S} \rangle$, which are given by

$$\begin{aligned}\mathbf{E}_{\mathrm{S}} &= \begin{bmatrix} \mathbf{S} & \mathbf{0} \end{bmatrix} \begin{bmatrix} \mathbf{S}^{\mathrm{H}}\mathbf{S} & \mathbf{S}^{\mathrm{H}}\mathbf{I} \\ \mathbf{I}^{\mathrm{H}}\mathbf{S} & \mathbf{I}^{\mathrm{H}}\mathbf{I} \end{bmatrix}^{-1} \begin{bmatrix} \mathbf{S}^{\mathrm{H}} \\ \mathbf{I}^{\mathrm{H}} \end{bmatrix} \\ \mathbf{E}_{\mathrm{I}} &= \begin{bmatrix} \mathbf{0} & \mathbf{I} \end{bmatrix} \begin{bmatrix} \mathbf{S}^{\mathrm{H}}\mathbf{S} & \mathbf{S}^{\mathrm{H}}\mathbf{I} \\ \mathbf{I}^{\mathrm{H}}\mathbf{S} & \mathbf{I}^{\mathrm{H}}\mathbf{I} \end{bmatrix}^{-1} \begin{bmatrix} \mathbf{S}^{\mathrm{H}} \\ \mathbf{I}^{\mathrm{H}} \end{bmatrix}, \end{aligned} \quad (4)$$

where $\mathbf{0}$ represents a zero vector. We choose $\mathbf{Q}_{\mathrm{SI}} = \mathbf{E}_{\mathrm{S}}$ to be the oblique projection operator of the PDC scheme as we aim to maintain the desired signal with the PS $\mathbf{S}$ while cancelling the SI signal with the PS $\mathbf{I}$ [19].

$$\begin{aligned}\mathbf{Q}_{\mathrm{SI}} &= \begin{bmatrix} \mathbf{S} & \mathbf{0} \end{bmatrix} \begin{bmatrix} \mathbf{S}^{\mathrm{H}}\mathbf{S} & \mathbf{S}^{\mathrm{H}}\mathbf{I} \\ \mathbf{I}^{\mathrm{H}}\mathbf{S} & \mathbf{I}^{\mathrm{H}}\mathbf{I} \end{bmatrix}^{-1} \begin{bmatrix} \mathbf{S}^{\mathrm{H}} \\ \mathbf{I}^{\mathrm{H}} \end{bmatrix} \\ &= \mathbf{S}\left[\mathbf{S}^{\mathrm{H}}\mathbf{I}^{\perp}\mathbf{S}\right]^{-1}\mathbf{S}^{\mathrm{H}}\mathbf{I}^{\perp}, \end{aligned} \quad (5)$$

where $\mathbf{I}^{\perp} = (\mathbf{E} - \mathbf{I}\,\mathbf{I}^{\mathrm{H}})$ with $\mathbf{E} = \begin{bmatrix} 1 & 0 \\ 0 & 1 \end{bmatrix}$. $\mathbf{I}^{\perp}$ has the properties: $\mathbf{I}^{\perp}\mathbf{I} = \mathbf{0}$ and $\mathbf{I}^{\perp}\mathbf{S} = \mathbf{S}$. This means $\mathbf{I}^{\perp}$ is a null-steering operator because it nulls everything in the interference space $\langle \mathbf{I} \rangle$ while maintaining the signal space $\langle \mathbf{S} \rangle$. In addition, the PS_s have the property of $\mathbf{S}^{\mathrm{H}}\mathbf{S} = 1$ and $\mathbf{I}^{\mathrm{H}}\mathbf{I} = 1$. As a result, the operator $\mathbf{Q}_{\mathrm{SI}}$ has the following properties:

$$\begin{aligned}\mathbf{Q}_{\mathrm{SI}}\mathbf{S} &= \mathbf{S}\left[\mathbf{S}^{\mathrm{H}}\mathbf{I}^{\perp}\mathbf{S}\right]^{-1}\mathbf{S}^{\mathrm{H}}\mathbf{I}^{\perp}\mathbf{S} = \mathbf{S} \\ \mathbf{Q}_{\mathrm{SI}}\mathbf{I} &= \mathbf{S}\left[\mathbf{S}^{\mathrm{H}}\mathbf{I}^{\perp}\mathbf{S}\right]^{-1}\mathbf{S}^{\mathrm{H}}\mathbf{I}^{\perp}\mathbf{I} = \mathbf{0}. \end{aligned} \quad (6)$$

The property $\mathbf{Q}_{\mathrm{SI}}[\mathbf{S}\ \ \mathbf{I}] = [\mathbf{S}\ \ \mathbf{0}]$ is the key to cancelling SI in the PDC scheme. Although the incoming signal $\mathbf{Y}_{in}$ of the PDC scheme consists of the desired signal and the SI signal, the product of the matrix $\mathbf{S}^{\mathrm{H}}\mathbf{Q}_{\mathrm{SI}}$ and $\mathbf{Y}_{in}$ can effectively preserve the desired signal, and cancel the SI signal at the same time. The detailed analyses will be presented in Section III. The PDC scheme at the relay node may consume some power. In this work, we assume that the power used by the PDC cancellation scheme is negligible compared to the power used for signal transmission. This assumption is reasonable because the power consumed by the PDC scheme is mainly for multiplying the incoming signal $\mathbf{Y}_{in}$ with the matrix $\mathbf{S}^{\mathrm{H}}\mathbf{Q}_{\mathrm{SI}}$ as shown in (17).

III. SIGNAL MODELING

A. RELAY-ASSISTED TRANSMISSION

In this article, we assume the channel coefficients $|h_{sr,l}|^2$ and $|h_{rd,l}|^2$ are independent and identically distributed (i.i.d.) exponential random variables. We have the following theorem.

Theorem 1: If $\mathbf{h}_{sr} = [h_{sr,1}, h_{sr,2}, \ldots, h_{sr,L}]$ where $h_{sr,l} \sim \mathcal{CN}(0, \Omega)$ (i.e. $|h_{sr,l}| \sim$ Rayleigh(Ω), $l = 1, \ldots, L$), and $\mathbf{H}_{sr} = [H_{sr,1}, \ldots, H_{sr,M}] =$ fft$(\mathbf{h}_{sr})$, where M is the number of sub-bands in the OFDM system, then $H_{sr,m}$, where $m = 1, \ldots, M$, are also Rayleigh random variables $|H_{sr,m}| \sim$ Rayleigh$(L\Omega/M)$ if $M \geqslant L$ [25].

Proof: A Rayleigh random variable $h_{sr,l} \sim \mathcal{CN}(0, \Omega)$ with $\mathbb{E}\{|h_{sr,l}|^2\} = 1$ can be considered as a Nakagami-m random variable, i.e., $h_{sr,l} \sim$ Nakagami-m$(1, \Omega)$. It is known that $|H_{sr,m}|$ follows Nakagami-m(k', Ω'), where $k' = L/(L-1+1) = 1$ and $\Omega' = (1/M)\sum_{l=1}^{L-1}\Omega = L\Omega/M$ [26]. Thus, $|H_{sr,m}| \sim$ Rayleigh$(L\Omega/M)$ [25].

From *Theorem* 1, it is clear that $X = |H_{sr,m}|^2$ and $Y = |H_{rd,m}|^2$ are exponentially distributed random variables. We set the mean values of X and Y are λ_s and λ_d respectively. The probability density function (PDF) $f_X(x)$ of X, the cumulative distribution function (CDF) $F_Y(y)$ of Y and the cumulative distribution function $F_Z(z)$ of $Z = XY$ can be

expressed as [9], [14]

$$f_X(x) = f_{|H_{sr,m}|^2}(x) = \frac{1}{\lambda_s} e^{-\frac{x}{\lambda_s}}, \tag{7}$$

$$F_Y(y) = \Pr(Y < y) = 1 - e^{-\frac{y}{\lambda_d}}, \tag{8}$$

$$F_Z(z) = 1 - 2\sqrt{\frac{z}{\lambda_s \lambda_d}} K_1\left(2\sqrt{\frac{z}{\lambda_s \lambda_d}}\right), \tag{9}$$

where $K_1(\cdot)$ is the first-order modified Bessel function of the second kind [27]. In this article, we consider the normalised channels for fair comparisons, thus $\lambda_s = 1$ and $\lambda_d = 1$.

Let us begin with the EH phase. Define $\mathbf{X}_e = [\mathrm{X}_{e,1}, \ldots, \mathrm{X}_{e,M}]$ as the original transmitted vector in the frequency domain which contains modulated energy symbols and $\mathbf{e} = [e_1, \ldots, e_M]$ as the transmitted symbol vector used to deliver energy from the source to the relay before cyclic prefix (CP) is added. The received base-band energy signal after CP removal at the relay is expressed as

$$\begin{aligned} \mathbf{y}_e &= \sqrt{\mathrm{P}_a}(\mathbf{e} \oplus \mathbf{h}_{sr}) + \mathbf{n}_e \\ &= \sqrt{\mathrm{P}_a}\big[\mathrm{ifft}(\mathrm{fft}(\mathbf{e}) .* \mathrm{fft}(\mathbf{h}_{sr}))\big] + \mathbf{n}_e, \end{aligned} \tag{10}$$

where $\mathrm{P}_a = \frac{\mathrm{P}_s}{d_1^\beta}$ and P_s represents the transmission power at the source, $\oplus$ represents cyclic convolution, $.*$ represents element-wise multiplication, $\mathbf{n}_e$ represents the white Gaussian noise (AWGN) at the relay with the variance of N_0, fft represents fast Fourier transform and ifft represents inverse fast Fourier transform. Then, the received signal in the frequency domain is

$$\mathbf{Y}_e = \mathrm{fft}(\mathbf{y}_e) = \sqrt{\mathrm{P}_a}(\mathbf{X}_e .* \mathbf{H}_{sr}) + \mathbf{N}_e, \tag{11}$$

where $\mathbf{X}_e = \mathrm{fft}(\mathbf{e})$, $\mathbf{H}_{sr} = \mathrm{fft}(\mathbf{h}_{sr})$ and $\mathbf{N}_e = \mathrm{fft}(\mathbf{n}_e)$. Using (11), the harvested energy $E_{h,m}$ for the m-th sub-carrier at the relay during αT time is given by [28]

$$E_{h,m} = \frac{\eta P_s |H_{sr,m}|^2}{d_1^\beta} \alpha T, \tag{12}$$

where $m = 1, \ldots, M$ and $0 < \eta < 1$ is the energy conversion efficiency. The relay transmitting power for the m-th sub-carrier is

$$P_{r,m} = \frac{E_{h,m}}{(1-\alpha)T} = \frac{\eta \alpha P_s X}{(1-\alpha) d_1^\beta}. \tag{13}$$

Now, we consider the FD information transmission phase. Denote $\mathbf{x} = [x_1, \ldots, x_M]$ as the transmitted information signal at the source before adding CP with the assumption of $\mathbb{E}\{|x_m|^2\} = 1$. Denote $\mathbf{z} = [z_1, \ldots, z_M]$ as the SI signal, which is the delayed version of $\mathbf{x}$ caused by the processing time of the relay. In the system with multipath transmissions, the desired received signal from the source transmitter and received SI signal from the local transmitter at the relay are denoted by $\mathbf{y}_{cp1}$ and $\mathbf{y}_{cp2}$ respectively. As a result, the overall received signal at the relay in the conventional system, i.e., without polarization, is given by

$$\mathbf{y}_r = \mathbf{y}_{cp1} + \mathbf{y}_{cp2} + \mathbf{n}_r, \tag{14}$$

where $\mathbf{n}_r$ is the white Gaussian noise (AWGN) at the relay with the variance of N_0.

As opposed to the conventional system, our system uses the dual-polarized antennas for transmission and reception. In particular, $\mathbf{x}_{cp}$ is polarized by the PS of the information signal $\mathbf{S}$, and $\mathbf{z}_{cp}$ is polarized by the PS of the SI signal $\mathbf{I}$. Thus, the desired received signal and SI signal have both horizontal and vertical components. The overall received signal at the relay in our system is represented as

$$\begin{aligned} \mathbf{y}_r &= \mathbf{S}\,\mathbf{y}_{cp1} + \mathbf{I}\,\mathbf{y}_{cp2} + \mathbf{n}_r \\ &= \begin{bmatrix} \mathbf{y}_{1H} \\ \mathbf{y}_{1V} \end{bmatrix} + \begin{bmatrix} \mathbf{y}_{2H} \\ \mathbf{y}_{2V} \end{bmatrix} + \begin{bmatrix} \mathbf{n}_H \\ \mathbf{n}_V \end{bmatrix}, \end{aligned} \tag{15}$$

where $\mathbf{y}_{1H}$, $\mathbf{y}_{2H}$ and $\mathbf{n}_H$ represent the horizontal components and $\mathbf{y}_{1V}$, $\mathbf{y}_{2V}$ and $\mathbf{n}_V$ represent the vertical components. After applying FFT to $\mathbf{y}_r$, the received OFDM symbol at the relay in the frequency domain is

$$\begin{aligned} \mathbf{Y}_{in} &= \mathrm{fft}(\mathbf{y}_r) \\ &= \begin{bmatrix} \mathrm{S}_1\sqrt{\mathrm{P}_a}\,\mathbf{X} .* \mathbf{H}_{sr} \end{bmatrix} + \begin{bmatrix} \mathrm{I}_1\big(\sqrt{\mathbf{P}_i} .* \mathbf{Z}\big) .* \mathbf{H}_{si} \\ \mathrm{I}_2\big(\sqrt{\mathbf{P}_i} .* \mathbf{Z}\big) .* \mathbf{H}_{si} \end{bmatrix} + \mathbf{N}_r \\ &= \mathbf{S}(\sqrt{\mathrm{P}_a}\,\mathbf{X} .* \mathbf{H}_{sr}) + \mathbf{I}(\sqrt{\mathbf{P}_i} .* \mathbf{Z} .* \mathbf{H}_{si}) + \mathbf{N}_r, \end{aligned} \tag{16}$$

where $\mathbf{X} = \mathrm{fft}(\mathbf{x})$, $\mathbf{H}_{sr} = \mathrm{fft}(\mathbf{h}_{sr})$, $\mathbf{Z} = \mathrm{fft}(\mathbf{z})$, $\mathbf{H}_{si} = \mathrm{fft}(\mathbf{h}_{si})$ and $\mathbf{N}_r = \begin{bmatrix} \mathrm{fft}(\mathbf{n}_H) \\ \mathrm{fft}(\mathbf{n}_V) \end{bmatrix}$. $\mathbf{P}_i$ is the power of the SI signal at the relay. $\mathbf{P}_i$ is assumed to be smaller than the transmitted power (by the relay) by 25 dB, where $\mathbf{P}_i = [P_{i,1}, \ldots, P_{i,M}]$, due to the difference in polarisation schemes as well as some passive SI cancellation techniques, such as absorptive shielding, circulator and directional isolation [29]. Then, $\mathbf{Y}_{in}$ is processed by the PDC scheme, which includes two main operations. Firstly, we use the oblique projection operator $\mathbf{Q}_{\mathrm{SI}}$ to maintain the desired signal and cancel the SI signal of $\mathbf{Y}_{in}$, i.e., $\mathbf{Q}_{\mathrm{SI}}[\mathbf{S} \quad \mathbf{I}] = [\mathbf{S} \quad \mathbf{0}]$. Secondly, we use $\mathbf{S}^{\mathrm{H}}$ to de-polarize the desired signal, i.e., $\mathbf{S}^{\mathrm{H}}\mathbf{S} = 1$. Thus, the output signal $\mathbf{Y}_{out}$ of the PDC scheme is given by

$$\begin{aligned} \mathbf{Y}_{out} &= \mathbf{S}^{\mathrm{H}}\mathbf{Q}_{\mathrm{SI}}\mathbf{Y}_{in} \\ &= \mathbf{S}^{\mathrm{H}}\mathbf{Q}_{\mathrm{SI}}\,\mathbf{S}(\sqrt{\mathrm{P}_a}\,\mathbf{X} .* \mathbf{H}_{sr}) \\ &\quad + \mathbf{S}^{\mathrm{H}}\mathbf{Q}_{\mathrm{SI}}\,\mathbf{I}(\sqrt{\mathbf{P}_i} .* \mathbf{Z} .* \mathbf{H}_{si}) + \mathbf{S}^{\mathrm{H}}\,\mathbf{Q}_{\mathrm{SI}}\,\mathbf{N}_r \\ &= \sqrt{\mathrm{P}_a}(\mathbf{X} .* \mathbf{H}_{sr}) + \boldsymbol{\mathcal{N}}_r, \end{aligned} \tag{17}$$

where $\boldsymbol{\mathcal{N}}_r = \mathbf{S}^{\mathrm{H}}\,\mathbf{Q}_{\mathrm{SI}}\,\mathbf{N}_r$ is the additional noise component caused by the PDC scheme, which has a variance of $\frac{MN_0}{2}$. After applying equalization to the signal $\mathbf{Y}_{out}$, we obtain $\mathbf{Y}_r$

$$\mathbf{Y}_r = \sqrt{\mathrm{P}_a}\mathbf{X} + \boldsymbol{\mathcal{N}}_r ./ \mathbf{H}_{sr}. \tag{18}$$

With the AF protocol, the power of the input signal for the m-th sub-carrier will be amplified at the relay by a factor $\xi_m^{\frac{1}{2}}$ which is given by

$$\xi_m = \frac{P_{r,m}}{\frac{P_s}{d_1^\beta} + \frac{N_0}{2}\frac{1}{X}}, \tag{19}$$

where the denominator $\frac{P_s}{d_1^\beta} + \frac{N_0}{2X}$ is the power constraint factor, i.e., the power of the received signal per sub-carrier at the relay using (18). Substitute (13) into (19), we obtain

$$\xi_m = \frac{2\alpha\eta P_s X^2}{(1-\alpha)(2P_s X + N_0 d_1^\beta)}. \tag{20}$$

Thus, the polarized received OFDM symbol at the destination after FFT is

$$\mathbf{Y}_p = \sqrt{d_2^{-\beta}}\,\mathbf{I}\big(\boldsymbol{\xi}^{\frac{1}{2}} .* \mathbf{Y}_r .* \mathbf{H}_{rd}\big) + \mathbf{N}_d, \tag{21}$$

where $\boldsymbol{\xi} = [\xi_1, \ldots, \xi_M]$, $\mathbf{H}_{rd} = \text{fft}(\mathbf{h}_{rd})$ and $\mathbf{N}_d = \begin{bmatrix}\text{fft}(\mathbf{n}_{dH})\\ \text{fft}(\mathbf{n}_{dV})\end{bmatrix}$ is the AWGN at the destination with variance of N_0, where $\mathbf{n}_{dH}$ represents the horizontal component and $\mathbf{n}_{dV}$ represents the vertical component. The signal $\mathbf{Y}_p$ then is de-polarized by $\mathbf{I}^{\text{H}}$. The received OFDM symbol at the destination after de-polarization and equalization is

$$\begin{aligned}\mathbf{Y}_d &= \Big[\sqrt{d_2^{-\beta}}\mathbf{I}^{\text{H}}\mathbf{I}\big(\boldsymbol{\xi}^{\frac{1}{2}} .* \mathbf{Y}_r .* \mathbf{H}_{rd}\big) + \mathbf{N}_d\Big]./\mathbf{H}_{rd}\\ &= \sqrt{d_2^{-\beta}}\Big[\boldsymbol{\xi}^{\frac{1}{2}} .* \big(\sqrt{\text{P}_a}\mathbf{X} + \boldsymbol{\mathcal{N}}_r./\mathbf{H}_{sr}\big)\Big] + \mathbf{N}_d./\mathbf{H}_{rd}\\ &= \underbrace{\sqrt{\frac{P_s\boldsymbol{\xi}}{d_1^{\beta}d_2^{\beta}}} .* \mathbf{X}}_{\text{signal}} + \underbrace{\sqrt{\frac{\boldsymbol{\xi}}{d_2^{\beta}}} .* \boldsymbol{\mathcal{N}}_r./\mathbf{H}_{sr} + \mathbf{N}_d./\mathbf{H}_{rd}}_{\text{noise}},\end{aligned} \tag{22}$$

In theory, as illustrated in (6) and (17), the oblique projection operator of the PDC scheme is able to completely cancel the SI signal. However, as a side effect, the cancellation scheme changes the power of the noise at the relay as shown in (17), which will impact the outage probability and throughput. As a result, the impact of the cancellation scheme is considered in the new noise term, indicated as $\sqrt{\frac{\boldsymbol{\xi}}{d_2^{\beta}}} .* \boldsymbol{\mathcal{N}}_r./\mathbf{H}_{sr}$ in (22). Thus, the instantaneous SNR of m-th sub-carrier at the destination is considered, which is denoted as $\gamma_D = \frac{\text{signal power}}{\text{noise power}}$. The expression of γ_D is represented as (23), as shown at the bottom of the page, where $X = |H_{sr,m}|^2$ and $Y = |H_{rd,m}|^2$.

B. OUTAGE PROBABILITY

In our system, the outage probability P_{out} is defined as the instantaneous system SNR γ_D in a sub-carrier being smaller than a threshold SNR γ_{th}, where $\gamma_{th} = 2^{R_{th}} - 1$ and R_{th} is the threshold transmission rate in *bits/sec/Hz*. Using (23), the outage probability is given by

$$\begin{aligned}P_{out} &= \Pr\{\gamma_D < \gamma_{th}\}\\ &= \Pr\left\{\frac{b_1X^2Y}{b_2X + c_1 + c_2XY} < 1\right\},\end{aligned} \tag{24}$$

where

$$\begin{aligned}b_1 &= 2\alpha\eta P_s^2,\\ b_2 &= \gamma_{th}2P_sN_0d_1^{\beta}d_2^{\beta}(1-\alpha),\\ c_1 &= \gamma_{th}N_0^2(d_1^{\beta})^2d_2^{\beta}(1-\alpha),\\ c_2 &= \gamma_{th}\alpha\eta N_0d_1^{\beta}P_s.\end{aligned} \tag{25}$$

The outage probability of our FD EH relaying system is calculated by two methods, which is then compared with that in the HD EH relaying system proposed in [12]. The corresponding time-switching architectures are shown in Fig. 3. The aim of deriving two different methods to compute the outage probability is to show a trade-off between accuracy, especially at low SNRs, and the computational simplicity of the two methods. Theoretically, Method 1 considers the distributions of the exponential random variables X and Y independently. This method is simpler than Method 2, i.e., Method 1 only involves a Bessel function, while Method 2 involves the integral of a Bessel function. However, Method 2 considers the product distribution of the independent random variables X and Y, which we believe is a better model for relaying systems as the outage probability of the source-relay link affects the outage probability of the relay-destination link in practice. The detailed expressions and analyses are elaborated as follows.

1) METHOD 1

This method directly employs the PDF of the exponential random variable X in (7) and the CDF of the exponential random variable Y in (8). Thus, the outage probability in Method 1 is

$$\begin{aligned}P_{out1} &= \Pr\left\{\frac{b_1X^2Y}{b_2X + c_1 + c_2XY} < 1\right\}\\ &= \Pr\left\{\left(b_1X^2 - c_2X\right)Y < b_2X + c_1\right\}\\ &= \begin{cases}\Pr\left\{Y < \dfrac{b_2X + c_1}{b_1X^2 - c_2X}\right\}, & X > \dfrac{c_2}{b_1}\\ 1, & X \leqslant \dfrac{c_2}{b_1}\end{cases}\\ &= \int_{\frac{c_2}{b_1}}^{\infty}\Pr\left(Y < \frac{c_1 + b_2x}{b_1x^2 - c_2x}\right)f_X(x)dx + \int_0^{\frac{c_2}{b_1}} f_X(x)dx\\ &= \int_{\frac{c_2}{b_1}}^{\infty}\left[1 - e^{-\frac{b_2x+c_1}{\lambda_d(b_1x^2-c_2x)}}\right]f_X(x)dx + \int_0^{\frac{c_2}{b_1}} f_X(x)dx\\ &= 1 - \frac{1}{\lambda_s}\int_{\frac{c_2}{b_1}}^{\infty} e^{-\left(\frac{b_2x+c_1}{\lambda_d(b_1x^2-c_2x)} + \frac{x}{\lambda_s}\right)}dx.\end{aligned} \tag{26}$$

The third equality in (26) follows from the fact that if $X \leqslant \frac{c_2}{b_1}$, then $b_1X^2 - c_2X$ will be a negative number and the probability of Y being greater than a negative number is always 1. Equation (26) involves the integral of an exponential function in terms of the computational complexity. To obtain the closed-form analytical result of the outage probability, we simplify (26) at high transmit SNRs. The factor $c_1 = \gamma_{th}N_0^2(d_1^{\beta})^2\,d_2^{\beta}(1-\alpha) \approx 0$ at a high SNR because the noise variance terms N_0^2 is negligible.

$$\gamma_D = \frac{\frac{P_s\xi_m}{d_1^{\beta}d_2^{\beta}}}{\frac{\xi_mN_0}{2d_2^{\beta}X} + \frac{N_0}{Y}} = \frac{2\alpha\eta P_s^2X^2Y}{2P_sN_0d_1^{\beta}d_2^{\beta}(1-\alpha)X + N_0^2(d_1^{\beta})^2d_2^{\beta}(1-\alpha) + \alpha\eta N_0d_1^{\beta}P_sXY}. \tag{23}$$

Using $\int_0^\infty e^{-\frac{\beta}{4x}-\gamma x}dx = \sqrt{\frac{\beta}{\gamma}}K_1(\sqrt{\beta\gamma})$ [27, §3.324.1], we obtain the approximated outage of Method 1 at high transmit SNRs as below

$$\tilde{P}_{out1} \approx 1 - \frac{1}{\lambda_s}\int_{\frac{c_2}{b_1}}^{\infty} e^{-\left(\frac{b_2}{\lambda_d(b_1x-c_2)}+\frac{x}{\lambda_s}\right)}dx. \quad (27)$$

We define a new variable $z \triangleq b_1x - c_2$.

$$\begin{aligned}\tilde{P}_{out1} &\approx 1 - \frac{1}{\lambda_s}\int_0^\infty e^{-\left(\frac{b_2}{z\lambda_d}+\frac{z+c2}{b_1\lambda_s}\right)}dz \\ &= 1 - \frac{e^{-\frac{c_2}{b_1\lambda_s}}}{b_1\lambda_s}\int_0^\infty e^{-\left(\frac{b_2}{z\lambda_d}+\frac{z}{b_1\lambda_s}\right)}dz \\ &= 1 - e^{-\frac{c_2}{b_1\lambda_s}}uK_1(u), \quad (28)\end{aligned}$$

where $u = \sqrt{\frac{4\,b_2}{b_1\lambda_s\lambda_d}}$ and $K_1(\cdot)$ is the first-order modified Bessel function of the second kind [27]. Thus, we obtain the closed-form expression of the approximated outage probability of Method 1.

In (28), the expression involves the Bessel function. Although (28) is relatively simple to compute numerically by common mathematical software packages such as MATLAB and MAPLE, it can be simplified further in high transmit SNRs using the series expansion of $uK_1(u)$ at $u = 0$ to approximate the Bessel function by a polynomial. The derived asymptotic line of the outage probability of Method 1 against the transmit SNR values can be represented as

$$\begin{aligned}P_\infty &= 1 - e^{-\frac{c_2}{b_1\lambda_s}}\left(\lim_{\text{SNR}\to\infty} uK_1(u)\right) \\ &= 1 - e^{-\frac{c_2}{b_1\lambda_s}}\Big(1 + \frac{1}{4}u^2(2\log(u) + 2\gamma - 1 - \log(4)) \\ &\quad + \frac{1}{64}u^4(4\log(u) + 4\gamma - 5 - 4\log(2)) + O(u^6)\Big), \quad (29)\end{aligned}$$

where γ is the Euler-Mascheroni constant [30] and O is the Big-O notation [31].

2) METHOD 2

This method considers the product distribution of the independent random variables X and Y in (9). The outage probability in this approach is represented as

$$\begin{aligned}P_{out2} &= \Pr\left\{\frac{b_1X^2Y}{b_2X + c1 + c2XY} < 1\right\} \\ &= \begin{cases}\Pr\left\{XY < \dfrac{c_1 + b_2X}{b_1X - c_2}\right\}, & X > \dfrac{c_2}{b_1} \\ 1, & X \leqslant \dfrac{c_2}{b_1}\end{cases} \\ &= 1 - \frac{1}{\lambda_s}\int_{\frac{c_2}{b_1}}^{\infty} e^{-\frac{x}{\lambda_s}}\Big[vK_1(v)\Big]dx, \quad (30)\end{aligned}$$

where $v = 2\sqrt{\frac{c_1+b_2\,x}{\lambda_s\lambda_d(b_1\,x-c_2)}}$. The derivation of (30) is illustrated in Appendix A. The expression of the outage probability involves the integral of a product of an exponential function and a Bessel function. Finding a closed-form solution of the outage probability in this case is thus very challenging.

C. THROUGHPUT AND OPTIMIZATION

In the FD EH system with the AF protocol, the instantaneous throughput is defined as

$$R_{AF}(\alpha) = (1 - P_{out}^{AF})(1 - \alpha)R_{th}. \quad (31)$$

Using (28), if SNR $\to \infty$, $uK_1(u) \to 1$ we have the upper bound of the throughput

$$R_{up}(\alpha) = e^{-\frac{c_2}{b_1\lambda_s}}(1 - \alpha)R_{th}. \quad (32)$$

The optimal α could be obtained by solving the equation $\frac{dR_{AF}(\alpha)}{d\alpha} = 0$. The first derivative D_{AF} of the throughput is given in (33), as shown at the bottom of the page, where $\sigma_1 = \sqrt{\frac{N_0\,d_1^\beta d_2^\beta \gamma_{th}(1-\alpha)}{\lambda_s\lambda_d P_s\alpha\eta}}$. Thus, optimal α could be obtained by solving the following optimization problem

$$\begin{aligned}&\sigma_1K_0(2\sigma_1) = \alpha K_1(2\sigma_1) \\ &\text{subject to } 0 < \alpha < 1. \quad (34)\end{aligned}$$

However, because the Bessel function is involved in the analytical expression, finding a closed-form solution of α is difficult. Therefore, the optimal α will be numerically evaluated using the build-in function "solve" based on the given system parameters, including, source power P_s, energy harvesting efficiency η, source to relay distance d_1, relay to destination distance d_2, path loss exponent β, noise variance N_0, threshold SNR γ_{th}, mean value λ_s of the variable X and mean value λ_d of the variable Y.

IV. NUMERICAL RESULTS

In this section, we present simulation results to validate our previous analytical expression and investigate the influence of key system parameters, including the optimal time splitting factor α in the TSR protocol and the SNR in the transmitter, on the outage probability and throughput of the system. The optimal α is numerically obtained, which results in the maximum system throughput. The channels are Rayleigh fading channels which contain random values drawn from the standard normal distribution. The 1024-point FFT is used in the OFDM system. N_s OFDM symbols are transmitted in total. The instantaneous SNR of a sub-carrier at the destination is calculated and compared with the threshold SNR γ_{th}. The outage probability in the simulation is calculated as the number of times when the instantaneous SNR of a sub-carrier is smaller than the threshold SNR γ_{th} divided

$$D_{AF} = \frac{dR_{AF}(\alpha)}{d\alpha} = \frac{2N_0R_{th}d_1^\beta d_2^\beta\gamma_{th}e^{-\frac{N_0d_1^\beta\gamma_{th}}{2\lambda_sP_s}}(1-\alpha)(\sigma_1K_0(2\sigma_1) - \alpha K_1(2\sigma_1))}{\lambda_s\lambda_dP_s\alpha^2\eta\sigma_1}. \quad (33)$$

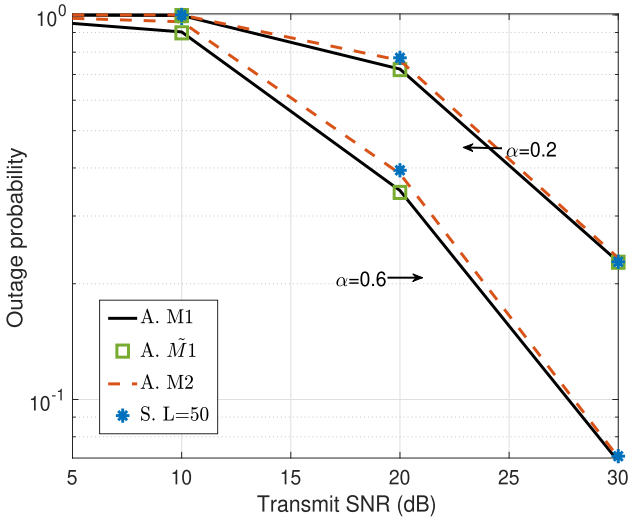

FIGURE 5. Outage probability vs. transmit SNR. Three analytical results compared with simulation in a FD system.

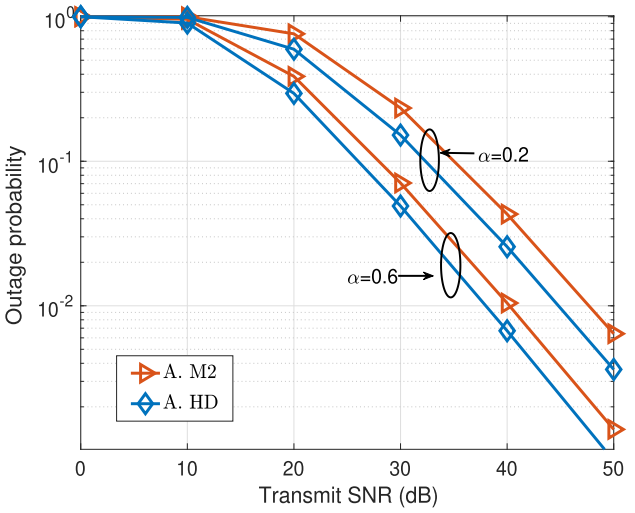

FIGURE 6. Outage probability vs. transmit SNR. The analytical result of Method 2 compared with analytical result in a HD system.

by the total numbers of transmitting symbols N_s. Unless otherwise stated, we set the targeted source transmission rate as $R_{th} = 3$ bps/Hz [9], [12], hence the outage SNR threshold is $\gamma_{th} = 2^{R_{th}} - 1 = 7$. The EH efficiency is set to $\eta = 0.9$. The path loss exponent is set to $\beta = 3$, which typically represents a path loss exponent in a wireless sensor network environment [32]. The mean values λ_s and λ_d are assumed to be one. We consider a small sensor network, where the direct link between the source and the destination is not available, for example, due to the obstructions. Therefore, a relay is deployed to assist their communications. For illustration, the source-to-relay and the relay-to-destination distances are set to $d_1 = d_2 = 1.2$ m, except in Fig. 11 where distances vary up to 4 meters. It is worth noting that the analyses, mentioned in this article, work for any distance values.

Figs. 5 and 6 show the outage probability with respect to the transmit SNR. The derived analytical expressions of Method 1 and its approximation (defined in figure as "A. $M1$" and "A. $\tilde{M}1$") are shown in (26) and (28) respectively. The analytical expression of Method 2 in (30) is shown in Figs. 5 and 6 as "A. $M2$". The simulation result of the FD system defined in figures as "S. L = 50" and the analytical result of the HD system defined as "A. HD".

Fig. 5 shows that the closed-form approximation result of Method 1 is accurate enough for calculating the system outage probability as it very close to the exact analytical results. Besides, Fig. 5 also shows that analytically the outage probability of Method 2 is slightly higher than the Method 1 when the transmit SNR is smaller than 30 dB especially in the large α ($\alpha = 0.6$) case. The similarity of these two methods is that the variables X and Y are considered to be independent since there are Rayleigh fading channels in our system. However, the difference is that the Method 1 considers the PDF and CDF of the variables separately, i.e., $\Pr\{Y < \frac{c_1+b_2 X}{b_1 X^2-c_2 X}\}$, while Method 2 constructs the product of two independent random variables to model the relaying system, i.e., $\Pr\{XY < \frac{c_1+b_2 X}{b_1 X-c_2}\}$. By comparing the analytical results with the simulation results, we find that Method 2 is more accurate than Method 1, i.e., the simulation result is much closer to Method 2, in the lower range of SNRs, while computationally more complex. Both methods have similar accuracy at high SNRs. This result means that in the relaying system, the theoretical expression of outage probability is more accurate if we consider the product distribution of X and Y, rather than the PDF and CDF of X and Y respectively.

Fig. 6 compares the outage probabilities in our FD EH relaying system and the HD EH relaying system in [12]. As shown in Figs. 2 and 3, if FD systems spend the same amount of time on EH as in HD systems, theoretically double amount of information can be transmitted in the former systems. This means the energy used to re-transmit each information symbol will be half than that in the HD counterpart. Thus, in Fig. 6, for a fair comparison, the transmitted power per OFDM symbol in FD systems at the relay is intentionally set to half of that in the HD systems. Fig. 6 shows that in 40 dB SNR, the outage probabilities of FD are 0.043 and 0.010 while those of HD are 0.026 and 0.007 respectively. The performance difference of the FD system and the HD system becomes smaller with an increase of α.

Fig. 7 plots the outage probability of analytical results and simulation results in the FD system for different values of α with the transmit SNR = 30 dB. The HD system is also plotted as the reference. The results show that with the increase of the number of multipath L, the system outage probability also increases. Besides, the simulation results match very well our theoretical results. In addition, the outage probability of the FD system is about 1.5 times higher than the HD system. Similar with Fig. 6, the reason for the HD communication being better than the FD communication in terms of the outage probability is that the HD consumes the same amount of harvested energy at the relay to transmit half the amount of information to the destination, compared with the FD. Note that although the HD system has a better outage probability,

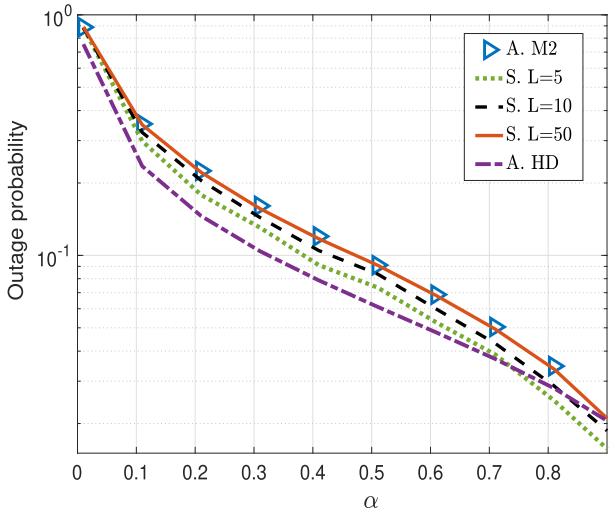

FIGURE 7. Outage probability vs. α for transmit SNR = 30 dB.

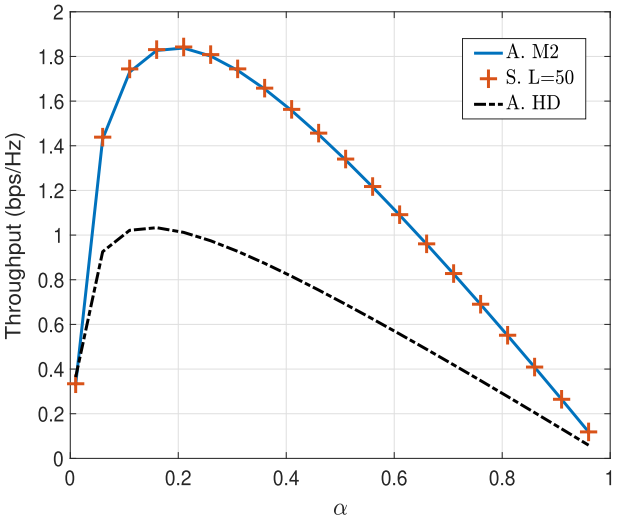

FIGURE 8. Throughput vs. α for transmit SNR = 30 dB.

its spectral efficiency and throughput are significantly lower than those in the FD system as detailed below.

Fig. 8 illustrates the throughput comparison between the HD scenario and the FD scenario with the transmit SNR = 30 dB. Fig. 7 shows that for both FD and HD systems, throughput increase as α increases from 0 to the optimal α (0.2 for FD case and 0.16 for HD case) but later decreases from its optimal value. This is because less energy is harvested before the optimal α which results in a larger outage probability (cf. in (31)). On the other hand, more time is wasted on EH and less time is available for information transmission when α is greater than the optimal value. Thus, smaller values of throughput are observed when α is away from the optimal α value. In addition, when both the FD system and HD system choose their optimal α, the throughput of the former is 1.85 times than the latter even though the same amount of time is spent on EH. This figure also shows that the analytical result agrees with the simulation results. This verifies the analytical expression presented in (31).

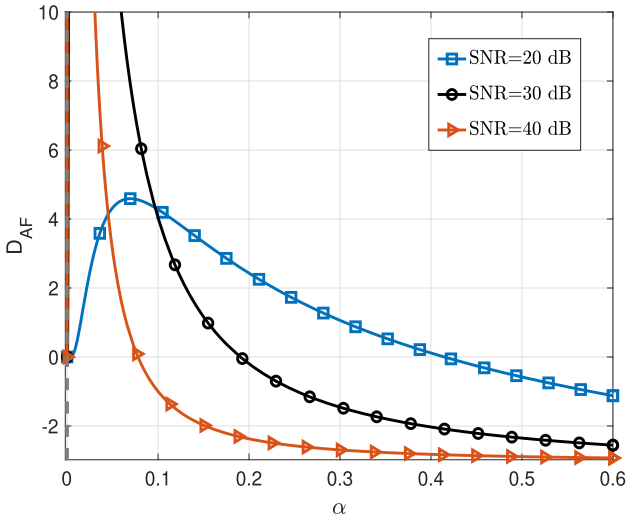

FIGURE 9. The first derivative of the throughput vs. α for the transmit SNR of 20, 30 and 40 dB.

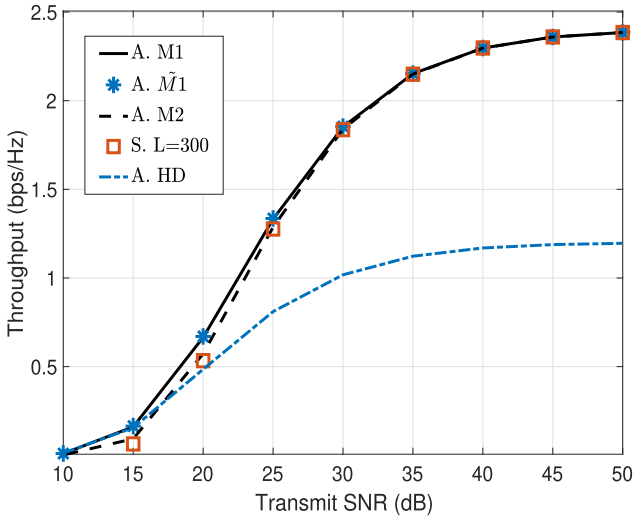

FIGURE 10. Throughput vs. transmit SNR for $\alpha = 0.2$.

Fig. 9 plots the first derivative of the FD system throughput (cf. in (33)) within the range $0 < \alpha < 1$. As shown in the figure, when $D_{AF} = 0$, we obtain the optimal α values, which are 0.41, 0.19, and 0.08 for transmit SNR values of 20 dB, 30 dB, and 40 dB respectively. This result shows that the optimal value decreases with the increase of the transmit SNR. Besides, the optimal value we obtained from the first derivative for the transmit SNR = 30 dB is consistent with the optimal alpha obtained in Fig. 8. Thus, it is clear that the optimal α can be numerically calculated by giving system parameters as shown in (34).

Fig. 10 illustrates the throughput performances of three analytical results for the FD system with the analytical throughput of the HD system serving as a benchmark. The derived analytical expressions of Method 1 in (26) and its approximation in (28) are denoted in this figure as "A. $M1$" and "A. $\tilde{M}1$" respectively. The expression of Method 2 in (30) is defined as "A. $M2$". This figure also shows the

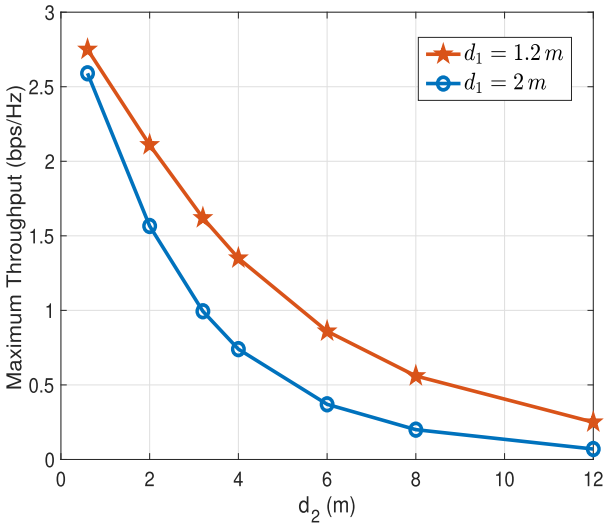

FIGURE 11. Maximum throughput vs. d_1 and d_2 for transmit SNR = 40 dB.

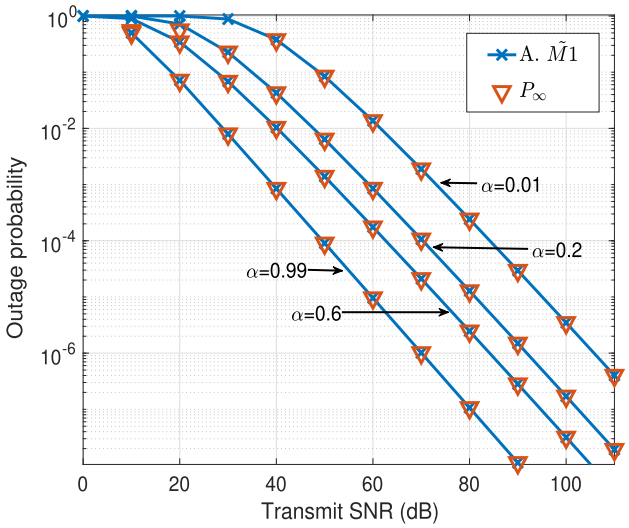

FIGURE 12. Validation of high SNR assumption. Outage probability for different α.

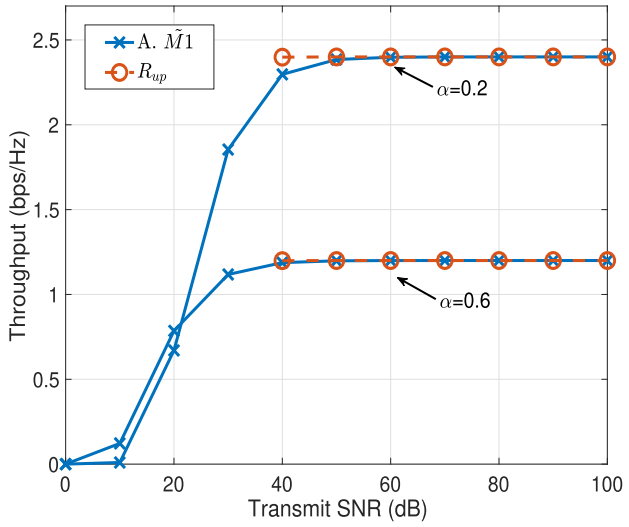

FIGURE 13. Validation of high SNR assumption. Throughput for different α.

simulated throughput of our FD system for $L = 300$. Referring to Figs. 5 and 10, Method 2 is seen to be a more accurate approach than Method 1 for both the outage probability and throughput when transmit SNR is less than 30 dB. When above 30 dB, all the theoretical results match the simulation results closely, so either approach would be accurate at high SNRs. From (13), it is clear that the relay transmitting power, i.e., the SI signal power, increases with the increase of transmit SNR. However, the superiority of the FD system over the HD counterpart is more significant when transmit SNR increases. In particular, the throughput gains of the FD system over the HD are 1.2, 1.85, and 1.95 at SNR values of 20, 30, and 50 dB, respectively. This result shows that, in FD systems, the PDC scheme can effectively cancel the loopback SI even when the power of the SI signal is high, which ensures the high system throughput. Besides, increasing the transmit SNR can improve more significantly the system throughput than in HD systems. Thus, it is important to research the throughput performance of FD systems in a high SNR regime.

Fig. 11 plots the system performances of the maximum throughput when considering different distances where d_1 is the source-to-relay distance and d_2 is the relay-to-destination distance. The maximum throughput is obtained when the optimal α is calculated by using (34). Fig. 11 shows that when d_1 is fixed the maximum throughput exponentially decreases with the increase of d_2 due to the impact of the path loss between the relay and destination. Besides, the difference between the two lines increases from 0.16 bps/Hz when d_2 equals to 0.6 m to a maximum value of 0.61 bps/Hz when d_2 equals to 4 m. Then, the gap narrows to 0.18 bps/Hz when d_2 equals to 12 m. The reason is that the increase of distance d_1 increases the path loss from the source to relay and decreases the harvested energy at the relay. Thus, the decrease of the maximum throughput is more significant for $d_1 = 2$ m than that of $d_1 = 1.2$ m when d_2 is relatively small, i.e., d_2 is less than 4 m. However, with the increase of d_2 so that the difference between $d_1 = 1.2$ m and $d_1 = 2$ m is negligible to d_2, the maximum throughput is mainly affected by the path loss from the relay to destination. Thus, the difference of the maximum throughput reduces in a large distance of d_2.

Figs. 12 and 13 illustrate the impact of α on the outage probability and the system throughput as well as validating the high SNRs assumption. The derived analytical expressions of the approximation of Method 1 and the asymptotic line of outage probability against the transmit SNR, are denoted as "A.$M1$" and "P_∞" respectively. Fig. 12 shows that the increase of the EH duration always improves the outage probability. Also, when SNRs are higher than 40 dB, the asymptotic line which uses the series expansion at $u = 0$ matches the approximation of Method 1. According to Figs. 5 and 12, we can conclude that, at high SNRs, the outage probability of the FD EH relaying system can be

accurately modeled using any of the theoretical Method 1, Method 1 approximation, series expansion, and Method 2. (cf. in (26), (28), (29) and (30), respectively). However, the theoretical Method 2 is preferred since it also matches the practice better at low SNRs. As shown in Fig. 13, the asymptotic line of throughput with a high transmit SNR assumption is defined in the figure as "R_{up}", which is the upper-bound of the system throughput. Note that the SNR in Figs. 10 and 13 is the transmit SNR, which is proportional to the transmit power, thus a high SNR regime is a reasonable range to be considered. Fig. 13 also shows that an increase of the EH duration slightly improves system throughput if SNRs are low. However, at high SNRs, the system throughput for the case $\alpha = 0.2$ outperforms the case $\alpha = 0.6$ since relay harvests enough energy from the transmitted signal and more time is spent on information transmission.

V. CONCLUSION

This article investigates an OFDM FD relaying system with no direct link from the source to the destination. A FD time switching-based relaying protocol is used to implement EH from the RF signals in the first phase as well as simultaneously receive and amplify-and-forward information in the second phase at the relay node. The performances of outage probability and throughput are evaluated for our FD system, in which the multipath propagated SI signals at the relay are eliminated by the PDC scheme. Specifically, the analytical expressions of the outage probability are derived in two different approaches over the Rayleigh frequency-selective fading channels, in which the approach considers product distribution of the source-relay channel and relay-destination channel is more accurate. Based on the mathematical expression of the system throughput, the optimal time split has also been derived to obtain the largest system throughput. In addition, comparing FD with HD relaying systems, the results show that the throughput of the former is nearly doubled than the latter at high transmit SNRs. For simplification, the asymptotic lines of outage probability and throughput are researched and validated at high SNRs.

The future work would be the extension of our proposed system to the case of multiple antennas [33], multiple users [34], and multiple relays [8]. We might also consider non-linear RF EH models [22], [23] and examine other SI cancellation techniques, such as the analog least mean square loops [35]–[38], to cancel the SI at the relay.

APPENDIX A
DERIVATION OF (30)

Using the definition of outage probability in (24), we have

$$P_{out} = \Pr\{\gamma_D < \gamma_{th}\}. \tag{35}$$

Substituting the instantaneous SNR in (23), the outage probability is

$$\begin{aligned} P_{out} &= \Pr\left\{\frac{b_1 X^2 Y}{b_2 X + c1 + c2XY} < 1\right\} \\ &= \Pr\left\{\left(b_1 X - c_2\right)XY < b_2 X + c_1\right\} \end{aligned} \tag{36}$$

where $X = |H_{sr,m}|^2$ and $Y = |H_{rd,m}|^2$. Utilizing the expression in (7) and (9), the system outage probability can be derived by Method 2

$$\begin{aligned} &P_{out2} \\ &= \begin{cases} \Pr\left\{XY < \dfrac{c_1 + b_2 X}{b_1 X - c_2}\right\}, & X > \dfrac{c_2}{b_1} \\ 1, & X \leqslant \dfrac{c_2}{b_1} \end{cases} \\ &= \int_{\frac{c_2}{b_1}}^{\infty} \Pr\left(Z < \frac{c_1 + b_2 x}{b_1 x - c_2}\right) f_X(x)dx + \int_0^{\frac{c_2}{b_1}} f_X(x)dx \end{aligned} \tag{37}$$

Using conditional probability, (37) can be rewritten as

$$\begin{aligned} P_{out2} &= \int_{\frac{c_2}{b_1}}^{\infty} F_Z\left(\frac{c_1 + b_2 x}{b_1 x - c_2}\right) f_X(x)dx + \int_0^{\frac{c_2}{b_1}} f_X(x)dx \\ &= \int_{\frac{c_2}{b_1}}^{\infty} \Big[1 - vK_1(v)\Big] f_X(x)dx + \int_0^{\frac{c_2}{b_1}} f_X(x)dx \\ &= 1 - \frac{1}{\lambda_s}\int_{\frac{c_2}{b_1}}^{\infty} e^{-\frac{x}{\lambda_s}}\Big[vK_1(v)\Big]dx, \end{aligned} \tag{38}$$

where $v = 2\sqrt{\frac{c_1 + b_2\, x}{\lambda_s \lambda_d (b_1\, x - c_2)}}$. This ends the derivation of (30).

REFERENCES

[1] O. Ozel, K. Tutuncuoglu, J. Yang, S. Ulukus, and A. Yener, "Transmission with energy harvesting nodes in fading wireless channels: Optimal policies," *IEEE J. Sel. Areas Commun.*, vol. 29, no. 8, pp. 1732–1743, Sep. 2011.
[2] J. Yang and S. Ulukus, "Optimal packet scheduling in an energy harvesting communication system," *IEEE Trans. Commun.*, vol. 60, no. 1, pp. 220–230, Jan. 2012.
[3] K. Tutuncuoglu and A. Yener, "Optimum transmission policies for battery limited energy harvesting nodes," *IEEE Trans. Wireless Commun.*, vol. 11, no. 3, pp. 1180–1189, Mar. 2012.
[4] D. Altinel and G. K. Kurt, "Diversity combining for RF energy harvesting," in *Proc. IEEE 85th Veh. Technol. Conf. (VTC Spring)*, Sydney, NSW, Australia, Jun. 2017, pp. 1–5.
[5] Z. Wang, J. Hu, J. Niu, J. Han, S. X. Wang, and J. He, "A novel magnetic energy harvester using spinning magnetoelectric transducer," *IEEE Trans. Magn.*, vol. 52, no. 7, pp. 1–4, Jul. 2016.
[6] J. Cannarella, J. Selvaggi, S. Salon, J. Tichy, and D.-A. Borca-Tasciuc, "Coupling factor between the magnetic and mechanical energy domains in electromagnetic power harvesting applications," *IEEE Trans. Magn.*, vol. 47, no. 8, pp. 2076–2080, Aug. 2011.
[7] Q. Zhang and E. S. Kim, "Micromachined energy-harvester stack with enhanced electromagnetic induction through vertical integration of magnets," *J. Microelectromech. Syst.*, vol. 24, no. 2, pp. 384–394, Apr. 2015.
[8] Q. N. Le, V. N. Q. Bao, and B. An, "Full-duplex distributed switch-and-stay energy harvesting selection relaying networks with imperfect CSI: Design and outage analysis," *J. Commun. Netw.*, vol. 20, no. 1, pp. 29–46, Feb. 2018.
[9] N. T. Do, Q. B. Vo Nguyen, and B. An, "A relay selection protocol for wireless energy harvesting relay networks," in *Proc. ATC*, Ho Chi Minh City, Vietnam, Oct. 2015, pp. 243–247.
[10] Y. Chen, "Energy-harvesting AF relaying in the presence of interference and Nakagami-m fading," *IEEE Trans. Wireless Commun.*, vol. 15, no. 2, pp. 1008–1017, Feb. 2016.
[11] K. Xiong, P. Fan, C. Zhang, and K. B. Letaief, "Wireless information and energy transfer for two-hop non-regenerative MIMO-OFDM relay networks," *IEEE J. Sel. Areas Commun.*, vol. 33, no. 8, pp. 1595–1611, Aug. 2015.
[12] A. A. Nasir, X. Zhou, S. Durrani, and R. A. Kennedy, "Relaying protocols for wireless energy harvesting and information processing," *IEEE Trans. Wireless Commun.*, vol. 12, no. 7, pp. 3622–3636, Jul. 2013.

[13] Y. Hu, N. Cao, and Y. Chen, "Analysis of wireless energy harvesting relay throughput in Rician channel," *Mobile Inf. Syst.*, vol. 2016, pp. 1–9, Oct. 2016.
[14] C. Zhong, H. A. Suraweera, G. Zheng, I. Krikidis, and Z. Zhang, "Wireless information and power transfer with full duplex relaying," *IEEE Trans. Commun.*, vol. 62, no. 10, pp. 3447–3461, Oct. 2014.
[15] Y. Dong, M. J. Hossain, and J. Cheng, "Performance of wireless powered amplify and forward relaying over Nakagami-*m* fading channels with non-linear energy harvester," *IEEE Commun. Lett.*, vol. 20, no. 4, pp. 672–675, Apr. 2016.
[16] P. N. Son, H. Y. Kong, and A. Anpalagan, "Exact outage analysis of a decode-and-forward cooperative communication network with N^{th} best energy harvesting relay selection," *Ann. Telecommun.*, vol. 71, nos. 5–6, pp. 251–263, Jun. 2016.
[17] S. Ikki and M. Ahmed, "Performance analysis of adaptive decode-and-forward cooperative diversity networks with best-relay selection," *IEEE Trans. Commun.*, vol. 58, no. 1, pp. 68–72, Jan. 2010.
[18] J. Li, L. C. Tran, and F. Safaei, "Performance evaluation of full-duplex energy harvesting relaying networks using PDC self-interference cancellation," in *Proc. IEEE ICSPCS*, Cairns, QLD, Australia, Dec. 2018, pp. 1–6.
[19] Y. Liu, C. Guo, Z. Zeng, and D. Li, "The polarization-enabled digital self-interference cancellation scheme for the full duplex communication," in *Proc. IEEE WPMC*, Sydney, NSW, Australia, Sep. 2014, pp. 414–418.
[20] T. Riihonen, S. Werner, and R. Wichman, "Hybrid full-duplex/half-duplex relaying with transmit power adaptation," *IEEE Trans. Wireless Commun.*, vol. 10, no. 9, pp. 3074–3085, Sep. 2011.
[21] J. Li, L. C. Tran, and F. Safaei, "Full-duplex OFDM relaying systems with energy harvesting in multipath fading channels," in *Proc. IEEE VTC-Fall*, Honolulu, HI, USA, Sep. 2019, pp. 1–5.
[22] E. Boshkovska, D. W. K. Ng, N. Zlatanov, and R. Schober, "Practical non-linear energy harvesting model and resource allocation for SWIPT systems," *IEEE Commun. Lett.*, vol. 19, no. 12, pp. 2082–2085, Dec. 2015.
[23] B. Clerckx, R. Zhang, R. Schober, D. W. K. Ng, D. I. Kim, and H. V. Poor, "Fundamentals of wireless information and power transfer: From RF energy harvester models to signal and system designs," *IEEE J. Sel. Areas Commun.*, vol. 37, no. 1, pp. 4–33, Jan. 2019.
[24] R. T. Behrens and L. L. Scharf, "Signal processing applications of oblique projection operators," *IEEE Trans. Signal Process.*, vol. 42, no. 6, pp. 1413–1424, Jun. 1994.
[25] L. C. Tran and A. Mertins, "Error performance and energy efficiency analyses of fully cooperative OFDM communication in frequency selective fading," *IET Commun.*, vol. 10, no. 18, pp. 2525–2533, Dec. 2016.
[26] Z. Kang, K. Yao, and F. Lorenzelli, "Nakagami-m fading modeling in the frequency domain for OFDM system analysis," *IEEE Commun. Lett.*, vol. 7, no. 10, pp. 484–486, Oct. 2003.
[27] I. S. Gradshteyn and I. M. Ryzhik, *Table of Integrals, Series, and Products*, 5th ed. New York, NY, USA: Academic, 1996.
[28] X. Zhou, R. Zhang, and C. K. Ho, "Wireless information and power transfer: Architecture design and rate-energy tradeoff," *IEEE Trans. Commun.*, vol. 61, no. 11, pp. 4754–4767, Nov. 2013.
[29] E. Everett, A. Sahai, and A. Sabharwal, "Passive self-interference suppression for full-duplex infrastructure nodes," *IEEE Trans. Wireless Commun.*, vol. 13, no. 2, pp. 680–694, Feb. 2014.
[30] J. Choi and H. M. Srivastava, "Integral representations for the euler-mascheroni constant γ," *Integral Transforms Special Functions*, vol. 21, no. 9, pp. 675–690, Mar. 2010.
[31] R. Vaz, V. Shah, A. Sawhney, and R. Deolekar, "Automated big-O analysis of algorithms," in *Proc. ICNTE*, Navi Mumbai, India, Jan. 2017, pp. 1–6.
[32] S. Kurt and B. Tavli, "Path-loss modeling for wireless sensor networks: A review of models and comparative evaluations," *IEEE Antennas Propag. Mag.*, vol. 59, no. 1, pp. 18–37, Feb. 2017.
[33] N. P. Le, L. C. Tran, and F. Safaei, "Energy-efficiency analysis of per-subcarrier antenna selection with peak-power reduction in MIMO-OFDM wireless systems," *Int. J. Antennas Propag.*, vol. 2014, pp. 1–13, Jun. 2014.
[34] Z. Ding and H. V. Poor, "Cooperative energy harvesting networks with spatially random users," *IEEE Signal Process. Lett.*, vol. 20, no. 12, pp. 1211–1214, Dec. 2013.
[35] A. Tuyen Le, L. C. Tran, and X. Huang, "Cyclostationary analysis of analog least mean square loop for self-interference cancellation in in-band full-duplex systems," *IEEE Commun. Lett.*, vol. 21, no. 12, pp. 2738–2741, Dec. 2017.
[36] A. T. Le, L. C. Tran, X. Huang, Y. J. Guo, and J. Y. C. Vardaxoglou, "Frequency-domain characterization and performance bounds of ALMS loop for RF self-interference cancellation," *IEEE Trans. Commun.*, vol. 67, no. 1, pp. 682–692, Jan. 2019.
[37] A. T. Le, L. C. Tran, X. Huang, and Y. J. Guo, "Beam-based analog self-interference cancellation in full-duplex MIMO systems," *IEEE Trans. Wireless Commun.*, vol. 19, no. 4, pp. 2460–2471, Apr. 2020.
[38] A. T. Le, L. C. Tran, X. Huang, and Y. J. Guo, "Analog least mean square loop for self-interference cancellation: A practical perspective," *Sensors*, vol. 20, no. 1, p. 270, Jan. 2020.

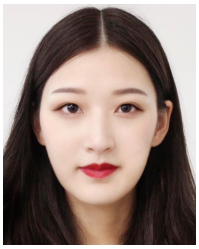

JIAMAN LI received the B.E. degree (Hons.) from the University of Wollongong, Australia, and Zhengzhou University, China, in 2016. She is currently pursuing the Ph.D. degree with the University of Wollongong. Her current research interest includes full-duplex communications in energy harvesting relaying networks.

LE CHUNG TRAN (Senior Member, IEEE) received the B.E. degree (Hons.) from the University of Transport and Communication (UTC), in 1997, the M.E. degree (Hons.) from the University of Science and Technology, Vietnam, in 2000, and the Ph.D. degree from the University of Wollongong (UOW), Australia, in 2006, all in telecommunications engineering. He was a Lecturer with UTC, from 1997 to 2012. From 2005 to 2006, he was an Associate Research Fellow with the Wireless Technologies Laboratory, UOW. From 2006 to 2008, he was a Postdoctoral Research Fellow with the University of Luebeck, Germany, under the Alexander von Humboldt (AvH) Fellowship. He has been with UOW, since 2009, where he is currently a Senior Lecturer. He has coauthored nearly 90 publications, including the book *Complex Orthogonal Space-Time Processing in Wireless Communications* (Springer), which is hold in 337 worldwide libraries. His research interests include 5G, MIMO, WBANs, positioning, navigation, and digital signal processing for communications. He has achieved the World University Services (WUS) Awards (twice), the Vietnamese Government's Doctoral Scholarship, the International Postgraduate Research Scholarship (IPRS), the Prestigious Humboldt Fellowships (twice), and the University Outstanding Contribution to Teaching and Learning (2019-OCTAL) Award. He has served as an Advisory Board Member for Cambridge Scholars Publishing; an Editorial Board Member for the *Electrical Engineering: An International Journal (EEIJ)*, a keynote Speaker for IEEE ICSPCS2019 Conference, an Organizing Committee Member (the Track Chair, the Session Chair, and the Publicity Co-Chair), and a Technical Program Committee (TPC) Member for over 30 IEEE conferences.

FARZAD SAFAEI (Senior Member, IEEE) received the Bachelor of Engineering (electronics) degree from the University of Western Australia and the Ph.D. degree in telecommunications engineering from Monash University, in 1998. He is currently the Chair of telecommunications engineering with the University of Wollongong. Before joining the University of Wollongong, he was the Manager of the Internetworking Architecture and Services Section, Telstra Research Laboratories. He was the Managing Director of the ICT Research Institute, from 2008 to 2013, and the Program Director of the Smart Services Cooperative Research Centre, Australia, from 2007 to 2014. His main research interests include multimedia signal processing and communications technology. He was the winner of a number of awards, including the Top Australian and Asia Pacific Awards for ICT Research and Development in 2012.